16th World Conference on Earthquake, 16WCEE 2017
Santiago Chile, January 9th to 13th 2017
Paper N° 2924
Registration Code: S-R1466059465

SHAKE TABLE STUDY ON THE SEISMIC RESPONSE OF MEDICAL EQUIPMENT ON WHEELS/CASTERS

F. Nikfar[1], D. Konstantinidis[2]

[1] Ph.D. Candidate, McMaster University, nikfarf@mcmaster.ca
[2] Assistant Professor, McMaster University, konstant@mcmaster.ca

Abstract

This paper presents an experimental investigation on the seismic response of medical equipment supported on wheels and casters. The test specimen was a large ultrasound machine, commonly found in hospitals. An extensive shake table testing program was carried out to understand and quantify the behavior of the equipment. The input signals for the shake table tests included floor motions of a four-story steel braced-frame hospital designed to satisfy seismic requirements of a site in the Los Angeles area. The results of the shake table tests reported in this paper include the seismic performance of the equipment under both unlocked and locked conditions, located on various floor levels of the building. It was observed that engaging the casters' locking mechanism does not necessarily decrease the relative displacement. The displacement response was sensitive to the excitation intensity and the orientation of the equipment with respect to the input excitation.

Keywords: medical equipment, nonstructural components, hospital, shake table testing

1. Introduction

Severe nonstructural damage and loss of functionality in medical facilities during the 1994 Northridge, 1995 Kobe, and 1999 Chi-Chi earthquakes resulted in impaired emergency response operations, demonstrating that the resilience of critical facilities, such as hospitals, is highly correlated to the seismic performance of their nonstructural components [1,2]. In fact, oftentimes the hospital building's structural system performs adequately, while the nonstructural components experience substantial damage [3,4], resulting in disruption in functionality [3,4].

The present study focuses on the seismic performance of wheel-supported and/or caster-supported EC, which are abundant in hospitals. About 30% of the hospital equipment and appliances are on wheels/casters due to mobility requirements [5]. The concern with equipment and appliances on wheels/casters during earthquakes is that they might exhibit large movements. Excessive movements could tear off or disconnect electric plugs and impair the functionality of the equipment. For instance, large movements of an anesthesia machine may not only tear off its electric plug, but also disconnect its connections to piped hospital oxygen, medical air, and nitrous oxide supplies. This would lead to malfunction of the equipment and possible loss of life. Large motion of EC in the operating room is also a big concern for doctors during operation. Moreover, large displacement increases the possibility of collision with other furniture, equipment, and surrounding partitions. Another adverse effect of excessive motion of EC during earthquakes is the possible blockage of safe egress routes. Impact as a result of collision introduces high accelerations that can lead to damage to acceleration-sensitive equipment and components. In the case of heavy equipment on wheels, a collision with people in vicinity of the equipment may result in injury.

A common seismic mitigation strategy for EC in science laboratories and other building types is tethering (using straps, chains, etc.). However, this practice has been shown to sometimes result in significant increase in accelerations, which may, in turn, result in damage to the equipment or even its contents (e.g., acceleration-sensitive biological samples in incubators) [6]. Base isolation is a seismic mitigation strategy that is becoming increasing popular for protecting both the structure and nonstructural components and systems of hospitals [5,7].

To date, there has been only one comprehensive experimental program that examined the performance of hospital equipment on wheels/casters [5,8,7]. It included full-scale shake table experiments of a four-story RC building at E-Defense to evaluate the performance of fixed-base and base-isolated medical facilities. Various rooms at different floor levels of the building were outfitted with hospital equipment and appliances to replicate realistic hospital rooms. The experimental program was aimed at studying various aspects of the facility. Shi et al. [7] focused specifically on the performance of items on casters. It was observed that the equipment with unlocked casters may experience movements as large as three meters. Multiple collisions with other equipment, furniture, and partitions were observed that resulted in accelerations up to 10 g. The experimental results of the base-isolated building showed that most equipment and appliances (including the ones with locked casters) experienced negligible movement except for those with unlocked casters that exhibited very large motions, leading to collisions with other equipment and surrounding partitions [7]. For equipment with locked casters, the response was very small when the building was tested as base-isolated, but when the building was tested as fixed-base, especially under near-fault ground motion, the equipment experienced the largest response and damage [7]. It appears that locking the casters is not one-size-fits-all solution, which calls for further investigation. Although these publications [5,8,7] reported very valuable qualitative observations from the shake table tests on the response of medical appliances, including ones on casters/wheels, the reported quantitative data was limited and did not allow extrapolation to other equipment on casters, e.g., estimation of their peak relative displacement and velocity and generation of fragility curves for this EC group.

In this study, the seismic response of an ultrasound machine housed in a conventional braced-frame hospital building, was investigated experimentally. The experimental program consisted of two phases. In the first phase, the frictional resistance of the wheels/casters was evaluated. This phase is not presented herein but the interested reader can refer to Nikfar [9]. In the second phase, shake-table experiments were performed using site-compatible ground and floor motions scaled to three earthquake intensity levels, i.e., maximum considered earthquake (MCE), design based earthquake (DBE), and service level earthquake (SLE)— chosen by the authors

to be 50% of DBE, intended to represent events that are more likely to occur over the lifetime of the building. The scaling factor of 0.5 is not intended to represent any particular return period but was chosen to quantify the response of the EC over a wider range of floor shaking intensity. The factor of 0.5 has also been used elsewhere, e.g. [10]. The floor motions at various levels of the building were generated from a series of nonlinear time history analyses. The shake table input excitation was unidirectional, and the equipment was placed in different orientations with respect to the excitation direction, both in locked and unlocked configurations. The motion of the equipment during the experiments was recorded using a combination of a vision-based measurement technique and accelerometers. The paper discusses in detail observations on the seismic response of the equipment under different testing conditions.

2. Nonlinear Time History of Hospital Building Model

A hypothetical four-story steel braced-frame hospital building located in Los Angeles, California, with site coordinates (34.02197°N , 118.28587°W) was designed according to the requirements of ASCE 7-05 [11] for Site Class C. The elevation and plan views of the building are shown in Fig. 1 (left). The mapped spectral accelerations are $S_S = 1.843$ g and $S_1 = 0.640$ g. The resulting DBE-level design spectrum is shown in Fig. 1 (right). The Steel Special-Concentrically-Braced-Frame (SCBF) lateral load resisting system for this building with hospital occupancy, i.e., Risk Category IV, and importance factor $I = 1.5$ was designed according to the requirements of IBC2006 [12], AISC360-05 [13], and ASCE 7-05 [11]. The SCBF was designed with a response modification factor, over-strength factor, deflection amplification factor, and drift ratio limit of $R = 6$, $\Omega = 2$, $C_d = 5$ and 1.5%, respectively. Further details on the building and the OpenSees model are presented in [9, 14].

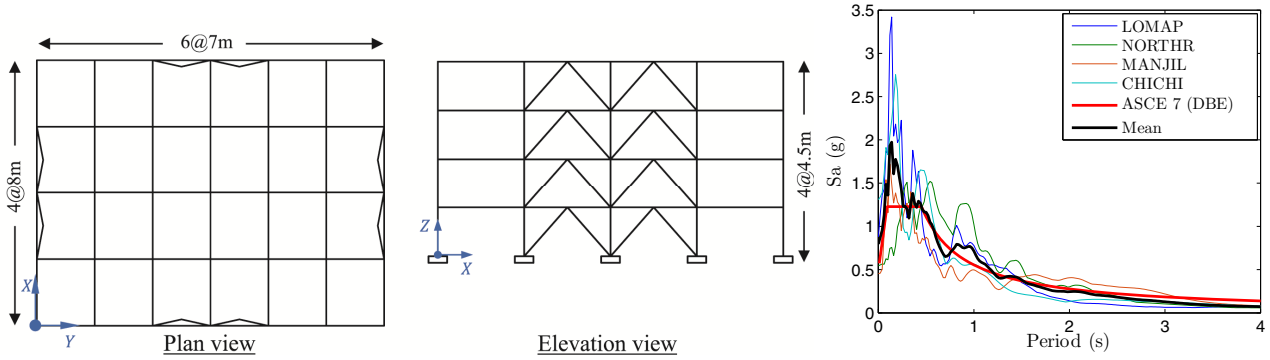

Fig. 1 – Left: plan and elevation views of the building. Right: acceleration response spectra for the scaled ground motions.

The vibration period in the first two modes was computed to be 0.54 s and 0.23 s, for the elastic structure. 2% Rayleigh damping, including both mass- and stiffness-proportional terms, was considered in the dynamic analysis of the model. The stiffness-proportional term of the damping was based on the last committed stiffness of the elements.

A set of four ground motions were selected from the PEER Strong Motion Database, NGA-West2, for the nonlinear time history analysis. The target design spectrum parameters $S_{DS} = 1.229$ g and $S_{D1} = 0.555$ g were used for spectrum-based ground motion selection. The Mean-Square-Error method with multiple period points from 0.1 s to 3.0 s was utilized in both the selection and the scaling of the ground motions. Only the H2 component of the recorded ground motions was considered in the scaling process. Properties of the selected ground motions and their corresponding scaling factors are listed in Table 1. Acceleration response spectra of the scaled ground motions are shown in Fig. 1. Both the horizontal (H2) and vertical components of ground motions were applied to the structure. Earthquake simulations were performed at the SLE (i.e., 50% DBE), DBE, and MCE levels. The analysis provided floor motions that were used subsequently in the shake table tests.

Table 1 – Ground motions used in this study, together with their scaling factors

ID	Scale Factor	Earthquake Name	Year	Station Name	Magnitude	V_{s30} (m/s)
LOMAP	1.34	Loma Prieta	1989	WAHO	6.93	388.33
NORTHR	1.06	Northridge-01	1994	Castaic - Old Ridge Route	6.69	450.28
MANJIL	0.91	Manjil	1990	Abbar	7.37	723.95
CHICHI	1.38	Chi-Chi Taiwan-03	1999	TCU129	6.2	511.18

3. Test Specimen

The test specimen discussed in this study was an ultrasound machine (procured from Hamilton Health Sciences), representing a typical heavy piece of medical equipment, supported on two wheels in the rear and two twin-wheel casters in the front, as shown in Fig. 2. The ultrasound was composed of three main parts: the main body (or case), the control panel, and the monitor. The main body housed most of the electronics and accounted for the majority of the mass of the equipment. The control panel and monitor were mounted flexibly on the main body, so that they could move and rotate depending on user needs. The dimensions and weight of the specimens are summarized in Fig. 2. The majority of the mass of the ultrasound was carried by the rear wheels, and the front casters were primarily for turning the machine. The ultrasound featured a brake mechanism acting on the front casters only. The brake mechanism was activated through a pedal engaging a positive braking system on the tread surface of both rubber tires of each twin-wheel caster. When the brake was engaged (referred to herein as 'locked' condition) the resistance to motion was significantly increased, but if sufficient force was applied, the wheel started rolling and the equipment moved; once in motion, the resistance dropped significantly. The pedal, however, was not designed to lock the swivel raceway of the caster; hence, the casters were free to rotate about the vertical pivot axis. The wheels in the rear of the ultrasound also featured rubber tires. Note that the rear wheels were always free to roll.

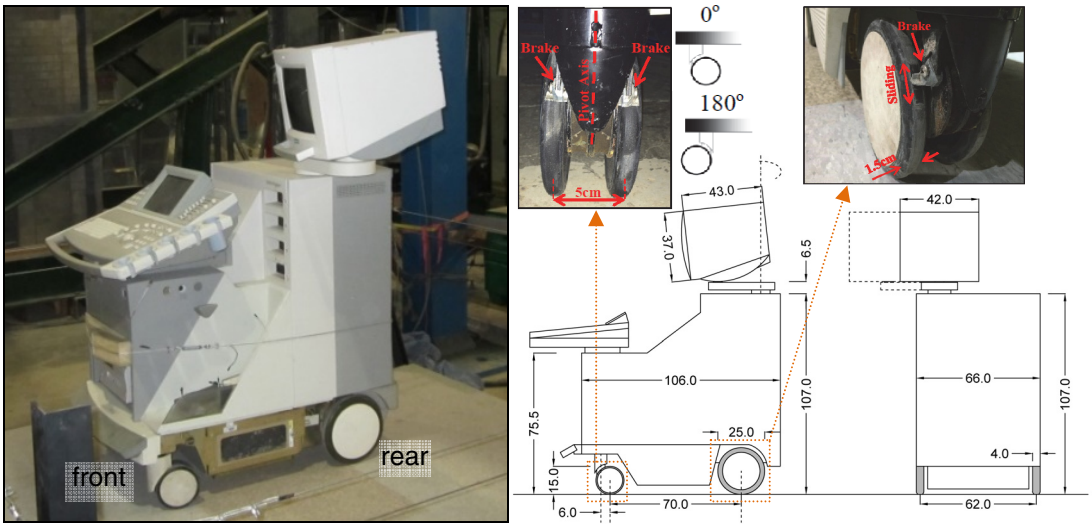

Fig. 2 – Ultrasound machine supported on wheels (rear) and twin-wheel casters (front). Dimensions in cm.

4. Shake Table Tests

The shake table at McMaster University, with displacement capacity of ±25 cm, made it possible to simulate a range of realistic floor motions to investigate the seismic response of the hospital equipment. The floor motions used as input for the shake table tests were generated by nonlinear time history analysis of an elaborate nonlinear structural model in OpenSees [15], details of which are presented in [9]. For the tests, the equipment was placed directly on the simulated hospital floor constructed on the shake table, as shown in Fig. 3. The methodology makes various assumptions and is constrained by limitations of the experimental facilities, e.g., ignoring the dynamic interaction between the equipment and the building, modeling assumptions in OpenSees, possible

collisions between the equipment and its surroundings, the effect of out-of-plane floor excitation, etc. In addition, the vertical component of the floor motion is not considered in this study since the shake table used is bidirectional (although only unidirectional tests were performed). However, it is noted that according to the results of the full-scale shake table tests at E-Defense [8], which did include vertical excitation, the horizontal movement of the EC on wheels and casters is not affected significantly by vertical floor excitation. This is due to the fact that, unlike in the case of sliding EC, the normal contact force does not contribute to the horizontal resistance of the wheels. Even a very low force would be adequate to overcome the resistance of the wheels and casters to rolling (which arises by friction between the caster's axle and roller or sliding bearings) in the unlocked condition. Even in cases where the casters were locked, the movement of the equipment was due to the sliding at the brake–tire contact points, rather than at the tire–floor contact points. Note that if the brakes are engaged and prevent the wheel from turning, the equipment will slide on the floor surface if the floor acceleration is strong enough to overcome the friction force at the tire–floor interface. In this case, the type of floor finish (e.g., vinyl, linoleum, terrazzo, etc.) and the vertical floor accelerations may influence the seismic response of the EC.

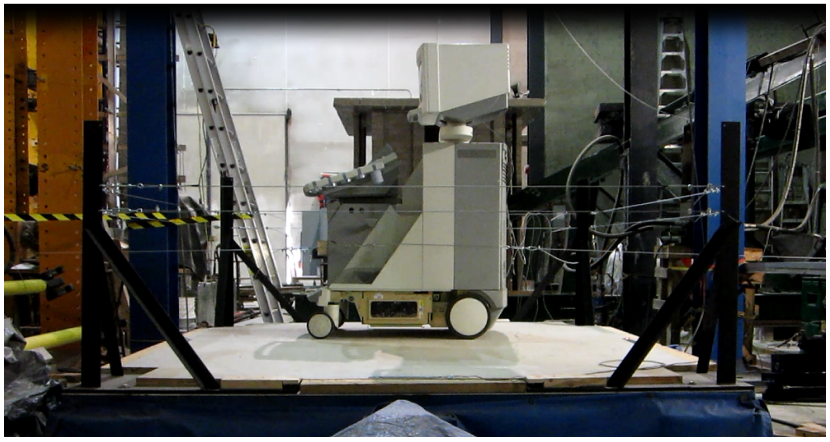

Fig 3 – Ultrasound machine on the shake table

The motion of the shake table in the horizontal direction was tracked using an accelerometer and a displacement sensor. Also, an additional accelerometer was attached to the inside of the ultrasound to measure the accelerations that internal electronic parts may experience during seismic shaking. As the motion of the equipment was expected to be complicated, a vision-based measurement system was used in lieu of conventional contact sensors. A video camera with a 2.7K (2704×1520 pixel) resolution at a 60 frames per second rate was used to track the motion of LED lights attached to the body and monitor of the ultrasound. In the case of the hospital cart, LED lights were attached to the rigid handle of the cart and also to the top of the smaller medical equipment on the cart to track relative displacements. Displacement and velocity response histories were computed from post-processing of the recorded frames. The accuracy of the vision-based measurements is approximately 0.5-mm and 3-cm/s for displacement and velocity, respectively. A detailed evaluation of the accuracy of the vision-based measurements in this study is presented in [16].

The shake table experiments were conducted using the ground, 1st, 2nd, and 3rd story motions as input. The ultrasound was tested under two conditions: with locked and with unlocked casters. Most of the tests were performed with the ultrasound's wheels parallel to the direction of excitation (see Fig. 2). For some tests, the equipment was rotated 45° (oblique) and 90° (perpendicular) to investigate the effect of equipment orientation. Table 2 summarizes the experimental program carried out in this study.

Table 2 – Shake table test matrix including the orientation of the equipment with respect to the shaking direction

Motion	Level	Ultrasound-unlocked (deg)			Ultrasound-locked (deg)			Hospital Cart (deg)		
		SLE	DBE	MCE	SLE	DBE	MCE	SLE	DBE	MCE
LOMAP	Ground	0	0,45,90	0	0	0,45,90	0	0	0,90	0,90
	1st	0	0	0	0	0	0	-	-	-
	2nd	0	0	0	0	0	0	-	-	-
	3rd	0	0,45,90	0	0	0,45,90	0	0	0,90	0,90
NORTHR	Ground	0	0,45,90	0	0	0,45,90	0	0	0,90	0,90
	1st	0	0	0	0	0	0	-	-	-
	2nd	0	0	0	0	0	0	-	-	-
	3rd	0	0,45,90	0	0	0,45,90	0	0	0,90	0,90
MANJIL	Ground	-	0	-	-	0	-	-	0	-
	3rd	-	0	-	-	0	-	-	0	-
CHICHI	Ground	-	0	-	-	0	-	-	0	-
	3rd	-	0	-	-	0	-	-	0	-

Note: the orientation angles are approximate

5. Shake Table Test Results and Discussion

5.1. Parallel to excitation

The responses of the ultrasound (i.e., body) and the attached monitor component in the horizontal plane *X*-*Y* were recorded using a motion-tracking technique [16]. The excitation for all the tests in this study was in the *X*-direction. Two LEDs were attached to the body and two to the monitor. Tracking the motion of two points (i.e., two LEDs) on the component provided a means to also measure the rotation (i.e., twisting) of that component about the vertical axis *Z*. Fig. 4 shows the absolute displacement of the ultrasound and its monitor (with respect to the floor) in the *X*-direction, together with the rotation due to the 3rd story motion corresponding to the NORTHR record at DBE level. The relative displacement is obtained by subtracting the position of the floor from the average position of the two LEDs attached on the ultrasound. Fig. 5 illustrates the *X*-*Y* plane relative displacement and relative velocity orbits (obtained by numerical differentiation) of the ultrasound under unlocked and locked conditions. The ultrasound is positioned parallel to the excitation. A small displacement is observed in the direction perpendicular to the excitation. Interestingly, in this particular example, the ultrasound exhibits larger displacement when the casters are locked than unlocked. Nevertheless, the relative velocity is smaller under the locked condition. The larger displacement under the locked condition is due to the fact that larger inertia forces and consequently larger accelerations can be transmitted to the ultrasound that can result in larger displacement responses. However, this is not always the case. The amplification in displacement due to addition of resistance is highly correlated to the characteristics of the input excitation [17]. For instance, if the floor acceleration cannot overcome the resistance, there will be no relative displacement/velocity whatsoever.

Fig. 6 shows the absolute acceleration response of the unlocked (top row) and locked (bottom row) ultrasound due to the 3rd story LOMAP-DBE excitation. The equipment experiences peak acceleration of about 0.1 g and 0.2 g under the unlocked and locked conditions, respectively. The figure also compares the acceleration histories recorded using the attached accelerometer (left column) to those derived from vision-based position measurements (right column).Vision-based acceleration results are based on twice-differentiated smoothed displacement using a first order Savitzky-Golay filter with a frequency resolution of 10 Hz. As it is evident in the figure, the high-frequency acceleration spikes recorded by the accelerometer were not captured in the acceleration history derived from displacement response. It should be noted that the accelerometer was attached on internal parts of the ultrasound, while the LEDs were attached on the case (i.e., body). Consequently, the difference between the plotted responses may be in part due to inherent differences in the dynamic response of the two points of the equipment. The vision-based acceleration history compares better with the accelerometer history in the case of the locked ultrasound, for which the equipment experienced larger accelerations. Overall,

the vision-based acceleration measurements provide a reasonable quantification of the accelerations experienced by the equipment.

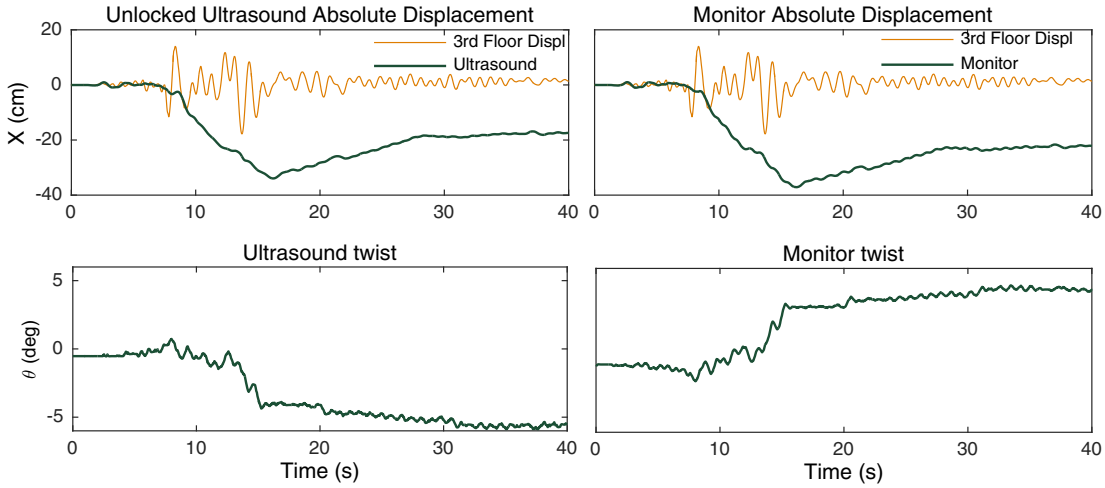

Fig. 4 – Absolute *X*-direction displacement and rotation of the unlocked ultrasound (left) and its monitor (right) under the 3rd story NORTHR-DBE excitation

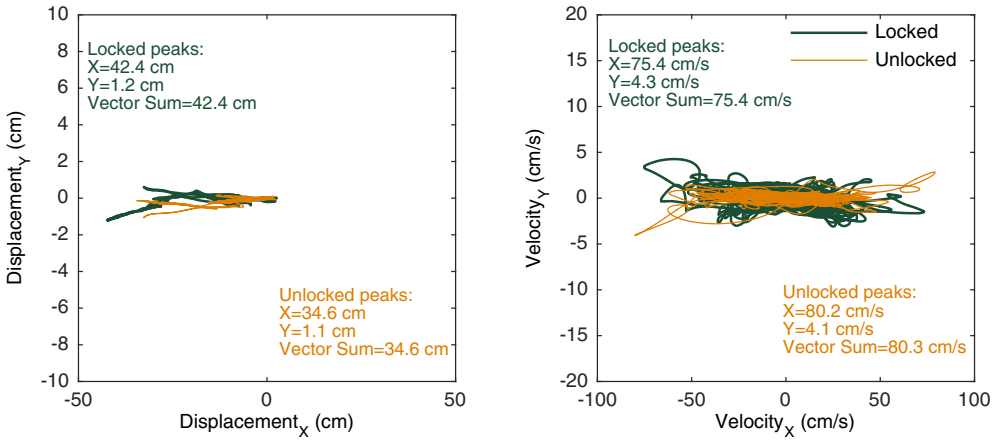

Fig. 5 – Relative displacement and velocity orbits of the locked and unlocked ultrasound under the 3rd story NORTHR-DBE excitation

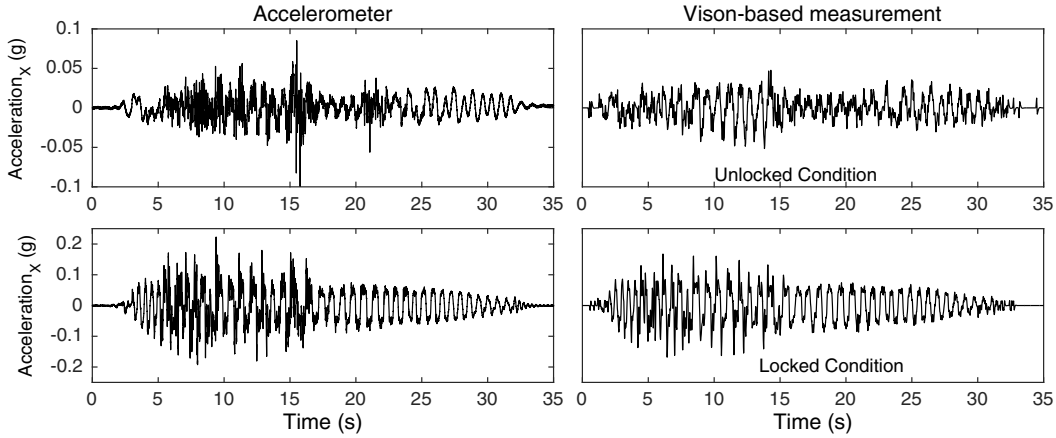

Fig. 6 – Absolute acceleration response of the ultrasound due to the 3rd story LOMAP-DBE excitation under locked (top) and unlocked conditions (bottom). Left: from accelerometer measurements. Right: from twice-differentiating the vision-based displacement measurements.

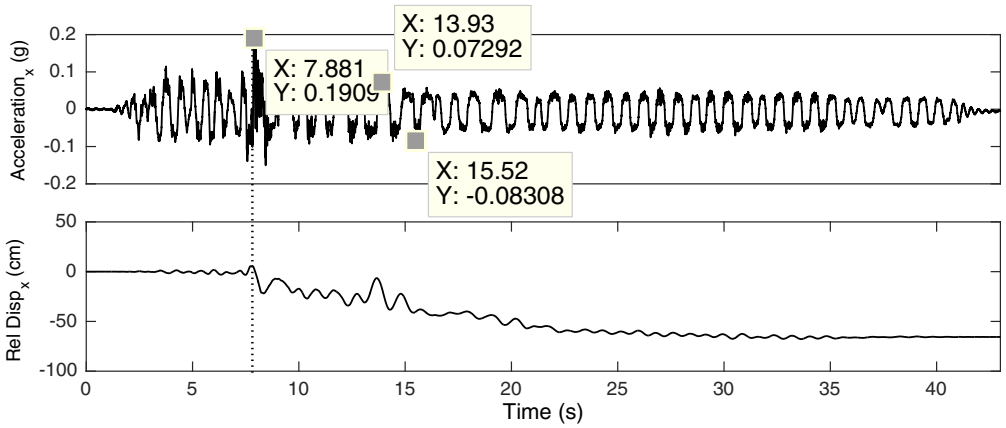

Fig. 7 – Estimation of the breakaway acceleration of the locked ultrasound, tested at 0-degree orientation under the 3rd story NORTHR-DBE excitation

As mentioned earlier, the frictional resistance of the locked ultrasound was not evaluated through cyclic testing. The absolute acceleration response can be used to provide a crude estimate of this resistance. Fig. 7 plots absolute acceleration and relative displacement response of the locked ultrasound subjected to the 3rd story NORTHR-DBE excitation. The major movement and peak acceleration occur at 7.8 s. Before this time, even though the equipment experiences vibrations with accelerations as large as 0.1 g, the casters' wheels do not actually rotate. An acceleration of 0.19 g is required for causing rigid-body motion (rather than vibration) of the locked ultrasound, evidenced by the subsequent drifting in the relative displacement (Fig. 7, bottom). This value, i.e., 0.19, can be thought of as breakaway friction coefficient. Thereafter, the ultrasound exhibits accelerations ranging from 0.05 g to 0.09 g. Fig. 8 shows the absolute acceleration of the monitor component in the *X*-direction, obtained using vision-based measurements from the LEDs attached on the monitor. The monitor experiences a peak acceleration of 0.44 g (vector sum).

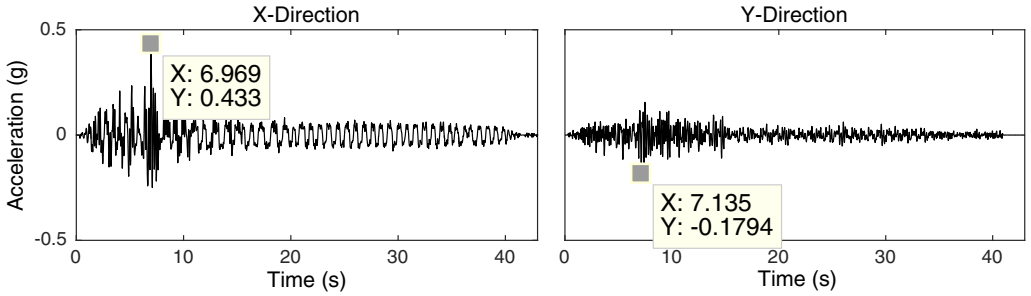

Fig. 8 – Absolute acceleration of the monitor of the locked ultrasound subjected to the 3rd story NORTHR-DBE motion. The vector sum of the acceleration in the X-Y plane is 0.44 g

5.2. Oblique to excitation

In order to investigate the effect of the excitation direction on the response, a number of tests were carried out with the ultrasound placed in an oblique orientation: as close as possible (visually but not measured precisely) to 45 degrees relative to the excitation direction (Fig. 10, right). Fig. 9 compares the relative displacement and velocity responses for the unlocked and locked ultrasound subjected to the 3rd story LOMAP-DBE excitation. As can be seen from the displacement plot, the ultrasound has the tendency to move merely in the rolling direction of the wheels. Although the locked ultrasound exhibits significantly smaller relative displacement than the unlocked ultrasound, it experiences slightly greater relative velocity. Fig. 10 plots the absolute acceleration response in the *X* and *Y* directions for the same experiment. The acceleration responses are comparable in

magnitude under locked and unlocked conditions due to the fact that, by rotating the equipment, the resistance increases in the direction of excitation since the wheels do not tend to slide in the direction perpendicular to rolling. The component of excitation in the direction perpendicular to rolling can excite the twist mode of response of the ultrasound. Large amount of rotation was observed in these tests. Fig. 11 compares the rotation for the unlocked and locked ultrasound. The unlocked ultrasound experiences a rotation as large as 35 degrees. The locked ultrasound rotated 16 degrees due to the fact that casters, even when locked, are free to rotate about their pivot.

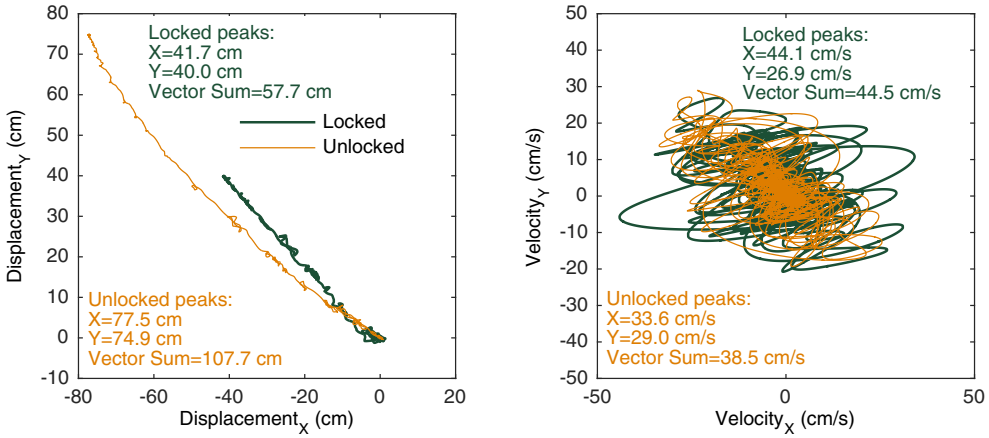

Fig. 9 – Relative displacement and velocity orbits of the locked and unlocked ultrasound tested in the 45-degree orientation relative to the input excitation: 3rd story LOMAP-DBE

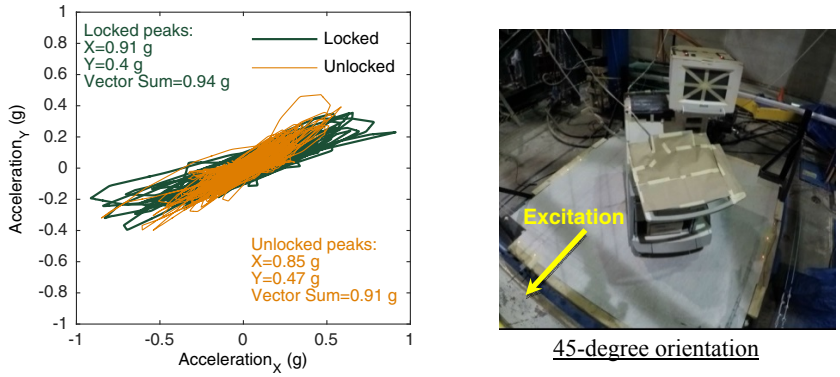

Fig. 10 – Absolute acceleration orbits of the locked and unlocked ultrasound tested in the 45-degree orientation relative to the input excitation: 3rd story LOMAP-DBE

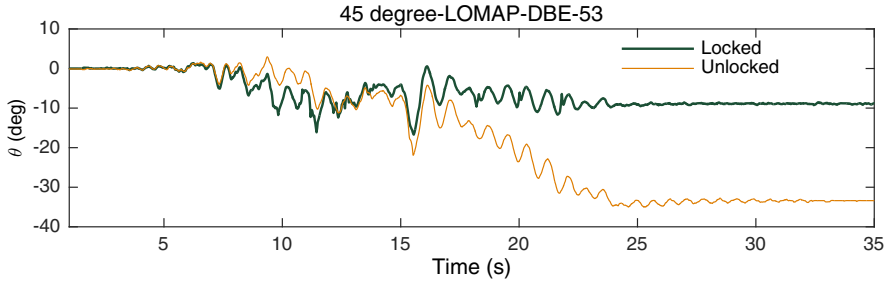

Fig 11 – Rotation of the locked and unlocked ultrasound tested in the 45-degree orientation relative to the input excitation: 3rd story LOMAP-DBE

5.3. Perpendicular to excitation

A number of experiments were performed with the ultrasound placed perpendicular to the excitation direction. Despite the slender aspect ratio of the ultrasound on the plane of the excitation, no notable rocking (i.e., uplift of the wheels) was observed under any of the 3rd story DBE-level motions. Similar to the tests carried out in the oblique orientation, the ultrasound tended to move along the rolling direction of the wheels. Although one may normally expect minimal movement in the direction perpendicular to the excitation, Fig. 12, which presents the response of the equipment in the perpendicular orientation, shows that this is not the case. Twisting of the ultrasound due to rotation of the casters about their pivot axes and lateral movement of the front side places the ultrasound in an oblique position with respect to the excitation; this creates an acceleration component in the direction parallel to the rolling direction of the wheels, causing motion of the equipment in perpendicular direction relative to the excitation. In this particular experiment, as shown in Fig. 12, the displacement of the unlocked ultrasound exceeded 120 cm, resulting in the ultrasound gently hitting the surrounding barrier built around the edges of the shake table. Fig. 13 shows the acceleration responses of the ultrasound case and monitor due to the 3rd story LOMAP-DBE excitation. The peak recorded vector-sum acceleration is approximately the same (about 1.2 g) under unlocked and locked conditions. The monitor, however, exhibited considerably larger acceleration (2.7 g) in the unlocked condition than in the locked condition (1.0 g). This significantly larger acceleration is attributed to rotational motion of the body of the ultrasound in the unlocked condition.

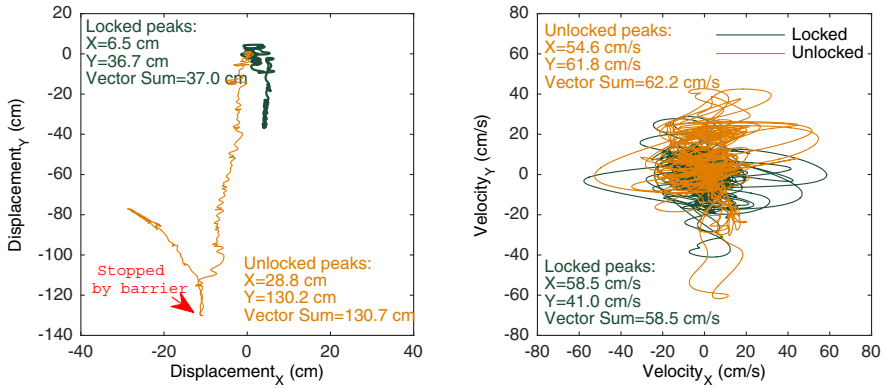

Fig. 12 – Relative displacement and velocity orbits of the locked and unlocked ultrasound tested in the perpendicular orientation relative to the input excitation: 3rd story LOMAP-DBE

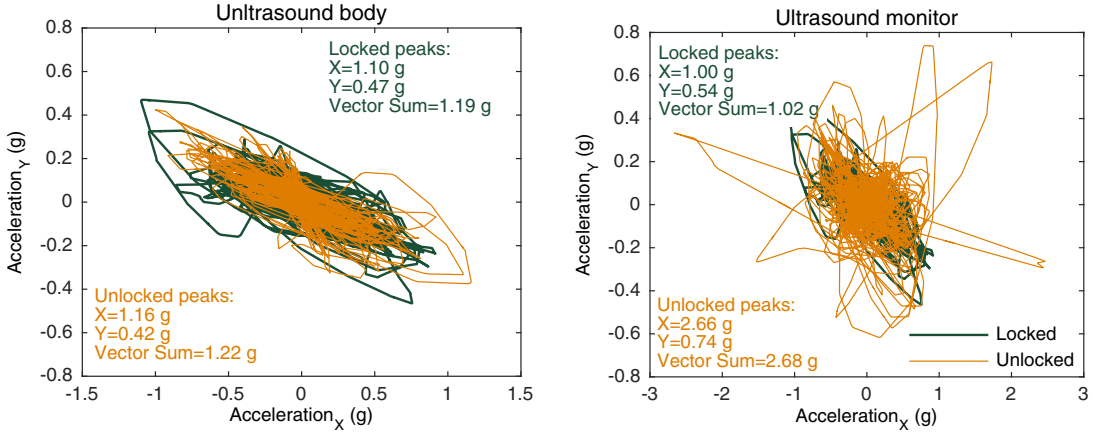

Fig. 13 – Absolute acceleration of the case and monitor of the locked and unlocked ultrasound tested in the perpendicular orientation relative to the input excitation: 3rd story LOMAP-DBE

5.4 Response in different story levels

Fig. 14 presents the peak relative displacement and velocity of the equipment items when they are placed in different stories of the building under SLE, DBE, and MCE earthquake intensities. In general, the relative displacement and velocity responses increase as the number of stories and input intensity increase; however, in some cases this observation does not hold. In some cases, the response changes very little in going from DBE to MCE, likely due to yielding of the building structure that limits the floor accelerations.

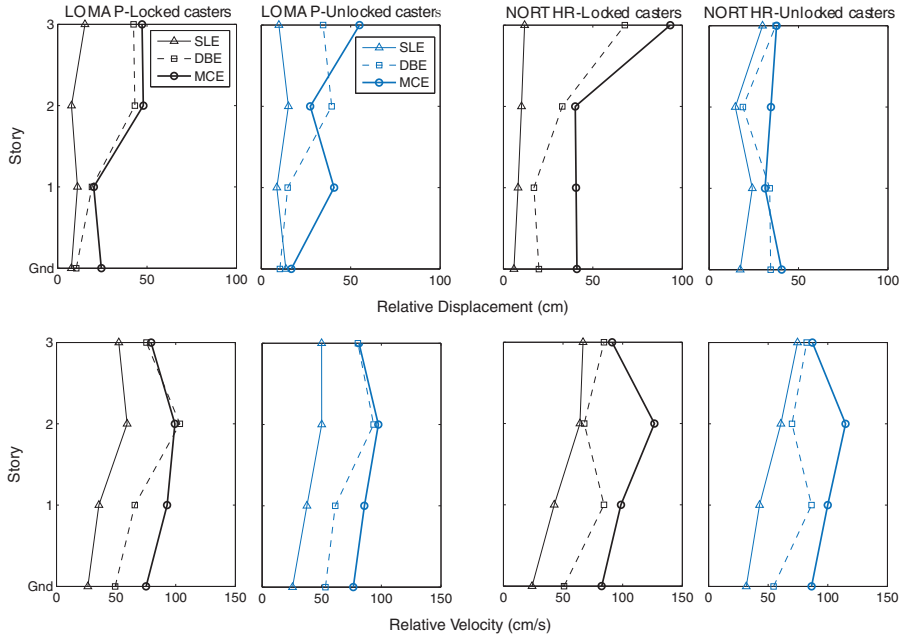

Fig. 14 – Peak demands on the ultrasound on different stories for the three hazard levels.

6. Conclusions

This study investigated the seismic response of hospital equipment on wheels and casters, located on various floor levels of a hypothetical four-story steel braced-frame hospital. The absolute acceleration response of the different floors of the building, computed using nonlinear time-history analysis of the building model in OpenSees, was used as input for the shake table tests. In addition to conventional accelerometers, a vision-based measurement system was utilized to quantify the complex motion of the equipment during the shake table tests. The performance of the equipment was evaluated at three intensity levels and for both unlocked and locked casters. Although the electronic functionality of the equipment was not assessed before/after the shake table test, there was no physical damage to the equipment (detachment of components or failure of any sort) as a result of the shaking. Furthermore, there was no notable rocking, and the main mode of response was rolling of the wheels and casters. It was observed that locking the casters can in some cases result in amplified response, depending on the input excitation intensity and orientation of the equipment with respect to the input excitation direction. While the general trend follows an increase in relative displacement and velocity at higher stories and input intensity, quite a few exceptions were observed. An interesting observation made was that, when equipment with casters and wheels was placed with the wheels perpendicular or at an oblique angle to the excitation direction, significant motion was observed in the direction the wheels were pointing towards.

7. Acknowledgements

The authors would like to gratefully acknowledge the financial support of the Natural Sciences and Engineering Research Council of Canada (NSERC). This paper presents selected results from a journal paper, currently considered for publication in *Earthquake Engineering and Structural Dynamics* [16].

8. References

[1] Cimellaro GP, Reinhorn AM, Bruneau M (2010): Seismic resilience of a hospital system. *Structure and Infrastructure Engineering*, **6**(1-2), 127-144.

[2] Filiatrault A, Sullivan T (2014): Performance-based seismic design of nonstructural building components: The next frontier of earthquake engineering. *Earthquake Engineering and Engineering Vibration,* **13**(1), 17-46.

[3] Mitrani-Reiser J, Mahoney M, Holmes WT, de la Llera JC, Bissell R, Kirsch T (2012): A functional loss assessment of a hospital system in the Bío-Bío province. *Earthquake Spectra*, **28**(S1), S473-S502.

[4] Miranda E, Mosqueda G, Retamales R, Pekcan G (2012): Performance of nonstructural components during the 27 February 2010 Chile earthquake. *Earthquake Spectra*, **28**(S1):S453-S471.

[5] Sato E, Furukawa S, Kakehi A, Nakashima M (2011): Full-scale shaking table test for examination of safety and functionality of base-isolated medical facilities. *Earthquake Engineering and Structural Dynamics*, **40**(13), 1435–1453.

[6] Comerio MC, Stallmeyer JC (2003): Laboratory equipment: estimating losses and mitigation costs. *Earthquake Spectra*, **19**(4), 779–797.

[7] Shi Y, Kurata M, Nakashima M (2014): Disorder and damage of base-isolated medical facilities when subjected to near-fault and long-period ground motions. *Earthquake Engineering and Structural Dynamics*, **43**(11), 1683–1701.

[8] Furukawa S, Sato E, Shi Y, Becker T, Nakashima M (2013): Full-scale shaking table test of a base-isolated medical facility subjected to vertical motions. *Earthquake Engineering and Structural Dynamics*; **42**(13), 1931–1949.

[9] Nikfar F (2016): Study of the Seismic Response of Unanchored Equipment and Contents in Fixed-Base and Base-Isolated Buildings. PhD Thesis, McMaster University.

[10] Yang T, Konstantinidis D, Kelly J (2010). The influence of isolator hysteresis on equipment performance in seismic isolated buildings. *Earthquake Spectra*, **26**(1):275–293.

[11] ASCE/SEI 7-05. Minimum design loads for buildings and other structures. American Society of Civil Engineers: Reston , Virginia, 2006.

[12] IBC2006-05. International Building Code (IBC). Falls Church 2005.

[13] ANSI/AISC 360-05. Specifications for structural steel buildings. Chicago: American Institute of Steel Construction; 2005.

[14] Nikfar F, Konstantinidis (2016). Shake table investigation on the seismic performance of hospital equipment supported on wheels/casters. Earthquake Engineering and Structural Dynamics (under review).

[15] McKenna F, Fenves GL, Scott MH (2000): Open system for earthquake engineering simulation (OpenSees) [Internet]. http://opensees.berkeley.edu.

[16] Nikfar F, Konstantinidis D (2016): Evaluation of vision-based measurements for shake-table testing of nonstructural components. *Journal of Computing in Civil Engineering* (ASCE) [in press].

[17] Nikfar F, Konstantinidis D (2016). Effect of the stick-slip phenomenon on the sliding response of objects subjected to pulse excitations. *Journal of Engineering Mechanics* (ASCE) (in press).